

Magnetic parameters, trace elements, and multivariate statistical studies of river sediments from southeastern India: a case study from the Vellar River

Marcos A. E. Chaparro · Mauro A. E. Chaparro ·
P. Rajkumar · V. Ramasamy · Ana M. Sinito

Received: 1 September 2009 / Accepted: 11 August 2010 / Published online: 25 August 2010
© Springer-Verlag 2010

Abstract This contribution constitutes a new study using magnetic parameters and trace element determinations of pollutants in river sediments from the Tamil Nadu state. The Vellar River covers a total length of about 200 km and flows into the Bay of Bengal. Sediment samples were collected at different sediment depths (up to 90 cm) from 12 sites to investigate their magnetic properties (27 samples) and the contents of trace elements (21 out of 27 samples) along the river; as well as to perform magnetic studies for various grain size fractions (16 sub samples). The magnetic results of magnetic susceptibility and remanent magnetizations suggest that the magnetic signal of these sediments is controlled by ferrimagnetic minerals magnetite-like minerals and a minor contribution of antiferromagnetic carriers (such as hematite minerals). Detailed studies of selected samples showed a higher magnetic concentration in finer grain-sized fractions and a slightly different magnetic mineralogy. Magnetic concentration-dependent parameters evidenced high values,

which, together with the background values, allowed us to identify magnetic enhancement at some sites. The Pearson correlation and multivariate statistical studies (Principal Component Analysis, Canonical Correlation Analysis) supported the relationship between the magnetic and chemical variables; in particular, magnetic susceptibility, anhysteretic and isothermal remanent magnetization are closely correlated to Co, Cr, Cu, Fe, V, Zn, and the pollution load index. In addition, Principal Coordinate Analysis and fuzzy C-means cluster analysis allowed us to make a classification and to perform a magnetic-chemical characterization of the data into four groups, thereby identifying critical (possibly polluted) sites from the Vellar River.

Keywords Environmental magnetism · Magnetic susceptibility · Fuzzy C-means clustering method · Pollution · River sediments

M. A. E. Chaparro (✉) · A. M. Sinito
Instituto de Física Arroyo Seco (UNCPBA), CONICET,
Pinto 399, B7000GHG Tandil, Argentina
e-mail: chapator@exa.unicen.edu.ar

M. A. E. Chaparro
Instituto Multidisciplinario de Ecosistemas y Desarrollo
Sustentable (UNCPBA), CONICET,
Pinto 399, B7000GHG Tandil, Argentina

P. Rajkumar
Department of Physics, Paavai Engineering College,
Pachal, Namakkal 637018, India

V. Ramasamy
Department of Physics,
Annamalai University, Annamalaiagar 608002,
Tamilnadu, India

Introduction

A large number of exhaustive studies of magnetic proxies for pollution have been conducted in different environments, including soils, sediments, and vegetation since the 1980s (e.g., Hunt et al. 1984; Thompson and Oldfield 1986; Beckwith et al. 1986). According to Petrovský and Ellwood (1999), atmospheric pollution is identified as one of the most harmful factors for ecosystems. Often, industrial and urban fly ashes include toxic elements and heavy metals; such airborne pollutants are diffused due to the atmospheric circulation. Land environments undergo a major impact because pollutants are transferred to the Earth's surface, made available, and taken up by organisms or incorporated into sediments.

Among the impacted environments, rivers and lakes from different countries have been studied using environmental magnetism. In the past years, several authors have focused on the magnetic properties of river and lake sediments and their relationship with heavy metals (e.g., Petrovský et al. 2000; Jordanova et al. 2004; Desenfant et al. 2004; Knab et al. 2006; Yang et al. 2007; Chaparro et al. 2008a). Although most of these studies proved the use of magnetic susceptibility for monitoring pollutants in river sediments, anhysteretic remanent magnetization (ARM) and related parameters may also be suitable tools under certain conditions. Such facts are based on correlations between magnetic parameters and heavy metals, such as, for example, Pb, Cr, and Zn (Scholger 1998); Pb and Zn (Desenfant et al. 2004); Ni, Cu, Zn, and the pollution load index (PLI, Chaparro et al. 2004); and Cu and Zn (Knab et al. 2006). Since bivariate statistical methods may not always yield significant results under certain conditions, Chaparro et al. (2008b) suggested applying other alternative multivariate statistical studies [such as canonical correlation analysis, principal coordinate analysis, linear discriminant analysis (LDA) and multivariate analysis of variance (MANOVA)] to validate the link between magnetic and chemical variables and to classify data according to the degree of contamination.

Previous magnetic investigations of river sediments from the Tamil Nadu state (southern India) were carried out on the Cauvery and Palaru rivers. The preliminary magnetic study on the Cauvery River by Ramasamy et al. (2006) revealed the predominance of magnetite minerals with different oxidation state and magnetic grain size distributions. Moreover, the magnetic concentration varied along the river, indicating magnetic enhancement associated with industrial pollution. In Chaparro et al. 2008a, a detailed magnetic and heavy metal study of river sediments from the Palaru and Cauvery Rivers was discussed. The work focused especially on magnetic parameters as pollution indicators from their relationship with contents of heavy metals; it obtained significant correlations (R values from 0.51 to 0.79 at 0.05 and 0.01 levels of significance) between concentration-dependent magnetic parameters (mass-specific magnetic susceptibility χ , ARM and saturation of isothermal remanent magnetization SIRM) and chemical variables (Zn, Ni, Cr, Fe and PLI). For this reason, the concentration-dependent magnetic parameters were identified as the best to describe heavy metal pollution in these Indian rivers. In addition, other multivariate statistical studies supported the relationship between variables and allowed the classification of critical (or possibly contaminated) sites.

In this contribution, we report new magnetic and pollution studies of river sediments from the Vellar River located in the Tamil Nadu state. This work contributes to

the knowledge obtained by previous studies of river sediments (Ramasamy et al. 2006; Chaparro et al. 2008a). Magnetic studies and chemical determinations are discussed to investigate the main magnetic carriers and pollutants concerning the influence of pollution sources. Different magnetic parameters were also analyzed as potential pollution indicators using biplots and statistical techniques.

Materials and methods

Study area and geological: hydrological setting

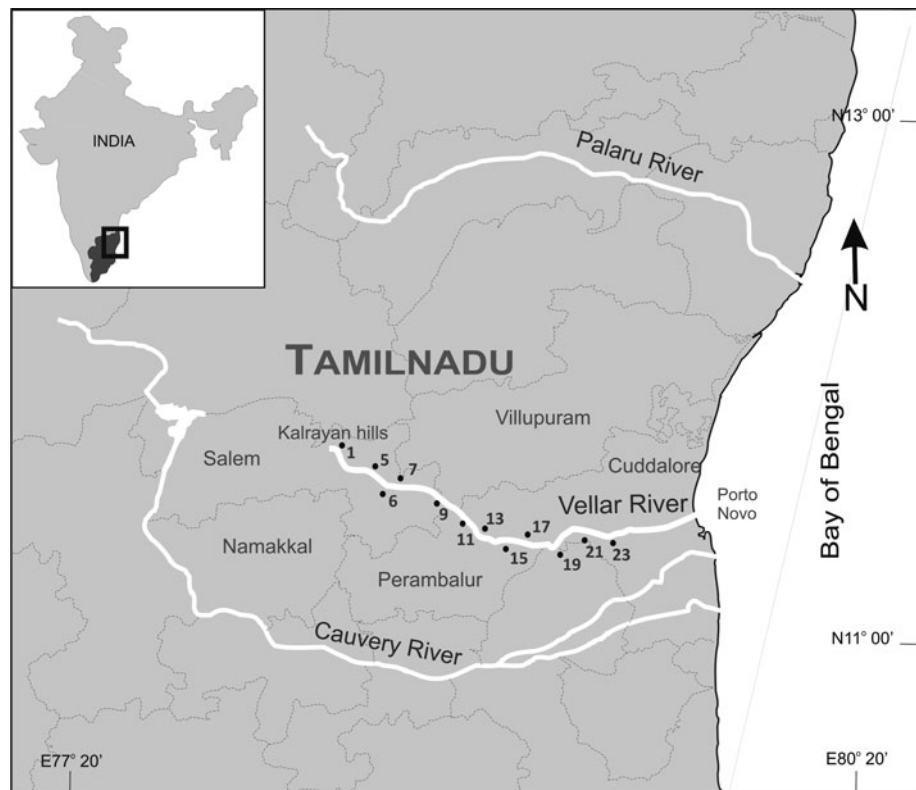
The Vellar basin is an important river basin in Tamil Nadu, situated between 11°13'N and 12°00'N and between 78°13'E and 79°47'E. The basin lies between Ponnaiyar River in the north and Cauvery River in the south with a total catchment area of 7,659 km² (Jain et al. 2007). For detailed information on the hydrology of the region, the reader is referred to Jain et al. (2007).

Over two-third of the basin comes under crystalline rocks of the Precambrian period, while the remaining comes under unconsolidated sediments of the Quaternary. The location of various districts in Tamil Nadu along with the Vellar River (the study area) is shown in Fig. 1. The study area comes under the Archaean complex of South India. The geological map and the field survey (Palanivel 2007) show that in this area three sets of rocks are present: pink granite, gneiss, and charnockite. The lithostratigraphic succession comprises (1) sand, silt, silty clay, and clay with kankar deposits (Recent to Sub-recent); (2) acid intrusives, pink granite, quartzo feldspathic gneiss, and charnockite (Archaean).

The Vellar River (Fig. 1) originates at the Kalrayan hills at an elevation of 900 m in the Salem district, runs for 90 km, and flows through the borders of the Villupuram and Perambalur districts for some few kilometers. In its last stretch, it enters the Cuddalore district, flowing for another 105 km, and ends its journey into the Bay of Bengal at Porto-Novo.

The elevation of the landscape of the Salem district generally ranges from 152 to 366 m above MSL with the exception of Yercaud which is at 1,524 m above MSL. Most of the soils of the district are clay, black loam, black sand, red ferruginous, and red sand. Black soil is due to alluvial deposits with red subsoil. Bauxite, dunite, magnetite, quartz, limestone, soapstone, and granite are important minerals available in the district. The district of Cuddalore lies on the east coast. Its southern boundary follows the course of two rivers, the Vellar and the Coleroon. Most of the district is a flat plain sloping very gently to the sea on the east. The hills are only on the

Fig. 1 Area map of Tamil Nadu state. Top and bottom (up to 90 cm) sediments were collected from different sites along the Vellar River



southwestern border. Black soil is the predominant soil type in this district. Red loam and red sandy soil are the other types of soil prevalent in the district. Sandy coastal alluvium soil occupies the coastal stretches of the district. There are lignite deposits mostly in sub-surface deposits (from 100 m to depths deeper than 300 m) and as part of Tertiary formations.

Geochemical studies were carried out by Palanivel (2007), to evaluate the general trends of the chemical compositions of fresh and weathered rocks of pink granite, hornblende, biotite gneiss, charnockite, and granite gneiss of the Vellar basin. These studies indicated homogeneous chemical compositions.

The Vellar basin experiences a tropical monsoon climate, with much variation in temperature, humidity, and evaporation through the year. During the summer months the maximum temperature is reported to be 40°C, whereas in winter months the minimum temperature goes down to 20°C. The monsoon season in the basin is from June to September during which significant rainfall is observed in the basin. The mean annual rainfall in the basin varies from 825 to 1,390 mm. Most of the rainfall in the basin occurs in the monsoon months and less rainfall occurs in non-monsoon periods (Jain et al. 2007).

Tamil Nadu is one of the most urbanized states of India, but it is still rural land; agriculture is the mainstay of life for about three-quarters of the rural population. The major industries of Tamil Nadu include cotton textiles, chemicals,

fertilizers, paper and paper products, printing and allied industries, diesel engines, automobiles and spare parts, cement, sugar, iron and steel, and railway wagons and coaches. The state of Tamil Nadu is the largest textile producer in India and is an important exporter of leather and cotton piece goods, tea, coffee, spices, tobacco, etc. There are a number of hydroelectric power stations in Tamil Nadu; the atomic power plant is located at Kalpakkam, in the Chengalpattu district.

The people living in these districts depend on this river for many purposes (irrigation, drinking and industries) and it is a source of minerals. Like other parts of Tamil Nadu, these districts also have hot weather that prevails during the months of April–May and a humid climate during the rest of the year except for December–February when it is slightly cold.

Sampling

The Vellar River covers a total length of about 200 km; twelve selected sites are shown in Fig. 1, and they were sampled and studied. All sediment samples were collected during the summer season in 2004. In seven sites, one 3–4 kg surface sample was collected from each, and in five sites, four samples (from the upper layer, from a depth of 30.5 cm, from a depth of 61.0 cm and from a depth of 91.4 cm) of about 3–4 kg were also collected from each site. For each sample, implements were properly cleaned

prior to sampling and a large amount of sediments (up to 4 kg) was collected to avoid contamination of the sample. The samples were sealed in polyethylene bags. The name of the sampling sites with latitude and longitude are given in Table 1.

In the laboratory, the samples were dried at room temperature in open air for a couple of days and stored in polyethylene bags. After that, dry samples were sieved (2 mm) to remove gravel fraction, and then they were packed, weighed, and labeled as samples V-1-0 to V-23-3 (where, e.g. V-1-0 stands for Vellar River, site 1, upper layer). Two selected samples (V-13-0 and V-23-0) were sieved (from 63 to 320 μm) and separated into fractions, namely, silt, fine and coarse sands. They were labeled as V-13-0-63/105/125/149/177/300/320/320+ and V-23-0-63/105/125/149/177/300/320/320+. Forty-three river sediment samples (27 collected samples + 16 sub-samples from sieved sediments) were sub-sampled for magnetic studies using plastic boxes (8 cm^3), and 21 (out of 27) samples were sub-sampled for chemical studies. All samples for magnetic studies were fixed using sodium silicate to prevent unwanted movements.

Magnetic measurements

Magnetic susceptibility, anhysteretic remanent magnetization, and isothermal remanent magnetization of acquisition (IRM) measurements were taken.

Magnetic susceptibility measurements were made using the magnetic susceptibility meter MS2 (Bartington Instruments Ltd.) linked to the MS2B dual frequency sensor (0.47 and 4.7 kHz). The volumetric susceptibility (κ), $\kappa_{\text{FD}}\%$ frequency-dependence ($\kappa_{\text{FD}}\% = 100 \times [\kappa_{0.47} - \kappa_{4.7}]/\kappa_{0.47}$), and mass-specific susceptibility were computed.

The ARM was imparted using a partial ARM (pARM) device attached to a shielded demagnetizer (Molspin Ltd.). The remanent magnetization was measured with a spinner fluxgate magnetometer (Minispin, Molspin Ltd.). Anhysteretic susceptibility (κ_{ARM}) was estimated using linear regression for ARM acquired at different DC bias fields (7.96, 47.75 and 71.58 A/m). The $\kappa_{\text{ARM}}/\kappa$ -ratio and the King's plot (κ_{ARM} vs. κ , King et al. 1982) were also studied.

IRM studies were performed using a pulse magnetizer model IM-10-30 (ASC Scientific). Each sample was magnetized by exposing it to growing stepwise DC fields, from 4.3 to 2,470 mT. The remanent magnetization after each step was measured using the aforementioned magnetometer Minispin. In these measurements, IRM acquisition curves and SIRM were determined using forward DC fields. Remanent coercivity (H_{CR} , the backfield required to remove the SIRM, or $\text{IRM} = 0$) and S -ratio ($= -\text{IRM}_{300\text{mT}}/\text{SIRM}$) were also calculated using backfield once the SIRM was reached.

Chemical analysis

Some samples were homogenized, quartered, and prepared for chemical analyses. Such samples were analyzed for nine elements: Ba, Co, Cr, Cu, Fe, Ni, Pb, V, and Zn. Analyses were performed by optic emission spectrometry, using an optic emission spectrometer by inductively coupled plasma (ICP-OES), Varian model 730-ES. The analytical method is US-EPA/600/R-94/111 (Method for the determination of metals in environmental samples Supplement 1. Method 200.7: "Determination of trace elements in waters and wastes by inductively coupled plasma—atomic emission spectrometry"). The samples were homogenized and the moist weights were determined with an analytic balance. The samples were dried at 60°C in an oven until the weights were constant. In order to maximize the homogeneity the dry samples were sieved through a polypropylene sieve. About 1 g of each homogenized and weighted sample was placed in a beaker with 4 ml of HNO_3 and 10 ml of HCl. The beaker was closed and placed on a heater at 95°C for 30 min. When the sample recovered to room temperature, it was placed in a 100-ml container and covered with ultra-pure water. The sample was left to settle over several hours to separate the insoluble material. The aqueous dissolution of each sample was analyzed by ICP-OES. The liquid sample was carried by a peristaltic pump to the humidifier system and was transformed to aerosol using argon gas. The aerosol was driven to the ionization zone, which is a plasma zone produced by the effect of an oscillating magnetic field, induced by a high-frequency current, on a flow of argon gas. The electrons of the different elements present in the sample were excited. When they returned from the excited state to the lowest available state, they radiated with characteristic energies according to the element. These radiations went through an optic system that classifies the radiation according to the wavelength. A detector measured the intensity of each radiation, which is related to the concentration of each element in the sample.

A pollution-related index, the PLI (Tomlinson et al. 1980), was studied. This index is defined using concentration factors (for details, see Chaparro et al. 2008a), i.e., the concentration of each metal and the baseline or the lowest concentration values detected for each metal in these sediment samples.

Statistical techniques

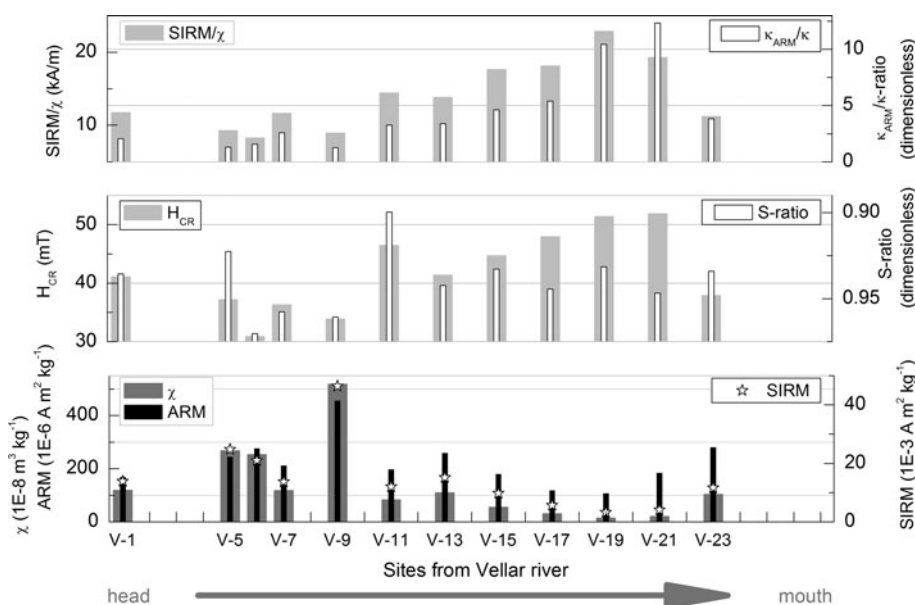
Bivariate and multivariate statistical analyses were performed using the software Multivariado InfoStat (InfoStat 2009) and the R free software (R version 2.9.2 © 2009). Among multivariate statistical analyses, canonical correlation analysis (CCA), principal component analysis (PCA),

Table 1 Sampling sites from the Vellar (V) River, south eastern India

Site	Location	Latitude (deg min)	Longitude (deg min)	Sample	Ba (mg kg ⁻¹)	Co (mg kg ⁻¹)	Cr (mg kg ⁻¹)	Cu (mg kg ⁻¹)	Fe (%)	Ni (mg kg ⁻¹)	Pb (mg kg ⁻¹)	V (mg kg ⁻¹)	Zn (mg kg ⁻¹)	PLI (dimensionless)
V-1	Thumbal	11°45'N	78°20'E	V-1-0	243	11	689	20	3.04	57	8	108	40	2.70
V-5	Yethapur	11°39'30"N	78°31'E	V-5-0	336	11	459	19	3.39	36	9	129	34	2.60
				V-5-1	314	10	365	12	3.26	25	8	122	31	2.20
				V-5-2	305	17	611	18	7.33	38	10	272	59	3.55
				V-5-3	347	8	401	13	1.91	51	10	75	20	2.08
V-6	Pethanayakkan-palayam	11°38'N	78°33'30"E	V-6-0	296	11	361	15	3.24	33	8	113	33	2.32
				V-6-1	-	-	-	-	-	-	-	-	-	-
				V-6-2	-	-	-	-	-	-	-	-	-	-
				V-6-3	-	-	-	-	-	-	-	-	-	-
V-7	Attur	11°36'N	78°36'30"E	V-7-0	267	9	289	12	2.50	27	5	79	26	1.80
V-9	Thalavasal	11°35'N	78°44'E	V-9-0	266	14	413	13	5.34	31	6	177	47	2.62
V-11	Pakkambadi	11°33'N	78°49'30"E	V-11-0	261	8	222	10	1.78	35	4	72	19	1.56
V-13	Korakkavadi	11°30'30"N	78°53'E	V-13-0	273	11	218	13	3.28	28	6	96	31	1.99
				V-13-1	206	24	422	13	9.74	43	6	163	75	3.13
				V-13-2	244	10	321	11	2.58	25	6	80	25	1.83
				V-13-3	249	9	511	11	2.20	24	4	70	20	1.72
V-15	Tholudur	11°26'N	78°59'E	V-15-0	240	12	383	9	3.05	29	4	81	26	1.85
V-17	Thitakkudi	11°24'30"N	79°07'E	V-17-0	217	7	269	10	1.72	20	2	64	16	1.29
V-19	Soundra-Solapuram	11°24'N	79°14'30"E	V-19-0	231	5	206	8	1.09	22	6	44	10	1.17
				V-19-1	-	-	-	-	-	-	-	-	-	-
				V-19-2	-	-	-	-	-	-	-	-	-	-
				V-19-3	-	-	-	-	-	-	-	-	-	-
V-21	Peralayur	11°27'N	79°21'E	V-21-0	250	6	291	8	1.68	32	6	57	14	1.47
V-23	Koodalayathur	11°25'N	79°28'E	V-23-0	264	11	275	9	3.37	33	4	103	32	1.93
				V-23-1	284	7	296	9	2.06	27	7	68	20	1.67
				V-23-2	256	6	217	7	1.96	20	9	68	16	1.47
				V-23-3	270	10	295	10	3.42	22	8	88	33	1.99
				Min.	206	5	206	7	1.09	20	2	44	10	1.17
				Max.	347	24	689	20	9.74	57	10	272	75	3.55
				Mean	267.6	10.3	357.8	11.9	3.23	31.3	6.5	101.4	29.9	2.05
				SD	36.1	4.2	128.7	3.6	2.02	9.7	2.2	51.5	15.5	0.60

Chemical studies for selected sediment samples (n = 21) from the Vellar River. Contents of nine elements and the PLI are listed. Samples depth_0: 0 cm; 1: 30 cm; 2: 60 cm; 3: 90 cm

Fig. 2 Magnetic results of surface sediments. Magnetic concentration-dependent parameters (χ , SIRM and ARM), magnetic carrier-dependent parameters (H_{CR} and S -ratio), and magnetic grain size-dependent parameters (SIRM/ χ -ratio and κ_{ARM}/κ -ratio) from the Vellar River



principal coordinate analysis (PCoordA), and the Fuzzy C-means Clustering method were studied.

The statistical studies were accomplished in order to get two aims: (1) the relationship between the magnetic and chemical variables; and (2) a data classification according to the degree of contamination. Twenty-one ($n = 21$) selected samples were investigated and the dataset included seven magnetic variables (χ , ARM, SIRM, S -ratio, H_{CR} , SIRM/ χ and κ_{ARM}/κ) and nine chemical variables (Ba, Co, Cr, Cu, Fe, Ni, Pb, V, and Zn). The variable PLI was only included for calculations in bivariate statistical studies.

Detailed information and the usefulness of these multivariate statistical methods for environmental magnetism studies can be found in Chaparro et al. (2006, 2008b); however, the main concepts and statistics in the multivariate analyses are briefly introduced. The CCA (Cuadras 1981) allows the investigation of the correlation between a set of variables X_i and another Y_i . Calculations for CCA were first made using all (seven) magnetic and the (nine) chemical variables, and then another three groups of magnetic variables (regarding magnetic feature/grain size/concentration-dependent variables) and the (nine) chemical variables were tried. On the other hand, although calculations and processes for PCA and PCoordA are similar the PCA uses the covariance or correlation (between variables) matrix to represent variables in the coordinate plane, while PCoordA is obtained from the distance (between individuals or cases) matrix. The PCA was carried out to study, in a multivariate way, the one-to-one relationships between the variables detailed earlier. For PCA, the data matrix was standardized with a column range, and then the covariance matrix (instead of the correlation matrix) was used to avoid overstated relationships in the graphic representation of the PCs. From PCoordA, it is

possible to achieve a graphic representation of the distance matrix and to search for similarities between cases, and hence, investigation of the existence of grouping with a homogeneous behavior is possible. According to the variability of magnetic and chemical data in this river, the Gower's distance (d_G , see Chaparro et al. 2008a) was used as a dissimilarity measure for the PCoordA. The Fuzzy C-means Clustering method allows us to get a fuzzy clustering using classification variables (in this work, magnetic M and chemical Ch variables).

Results and discussion

Magnetic carriers

Measurements of remanent magnetization revealed the dominance of ferrimagnetic carriers for Vellar samples (Fig. 2). Remanent coercivity values varied between 26.7 and 56.8 mT corresponding to magnetite-like minerals with different characteristics. An extra contribution of antiferromagnetic materials could be expected in samples with higher H_{CR} , which is in agreement with the acquisition IRM curves. As Fig. 3 shows, IRM values reach the SIRM between 300 and 500 mT, and not at fields <300 mT, as it to be expected for a magnetite population. Such behavior, as well as the higher H_{CR} values, may be explained from the presence of a subordinate magnetic phase. Chaparro et al. (2005) found, for example, that a high (total) H_{CR} value of 72.4 mT can be explained as a main magnetic phase of magnetite ($H_{CR1} = 47.5$ mT, contribution1 = 75.3%) and a subordinate phase of hematite ($H_{CR2} = 365.3$ mT, contribution2 = 24.7%).

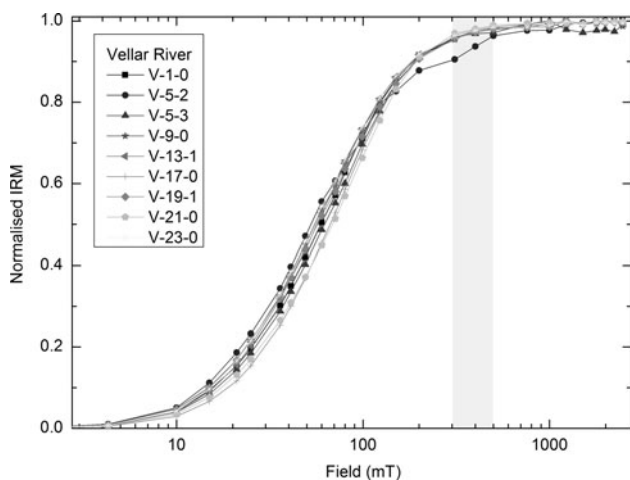


Fig. 3 Curves of acquisition IRM for selected samples

Values of $SIRM/\chi$ from 8.25 to 25.33 kA/m (Fig. 2) belong to the range of (titano) magnetite (Peters and Dekkers 2003) and higher values can be interpreted as a finer magnetic grain size in abundance.

Both magnetic parameters are displayed in a biplot (Fig. 4), where two groupings can be identified. The first grouping involves samples with softer magnetic carriers belonging to sites V-1/5/6/7/9/13/23. On the other hand, samples from sites V-11/15/17/19/21 belong to the second grouping; such samples show harder (or different) and finer magnetic carriers than the other samples.

The S -ratio values (between 0.90 and 1.00) clearly show the predominance of ferrimagnetic minerals for all samples (Fig. 2). However, there are differences among the samples indicating the presence of softer magnetic minerals for

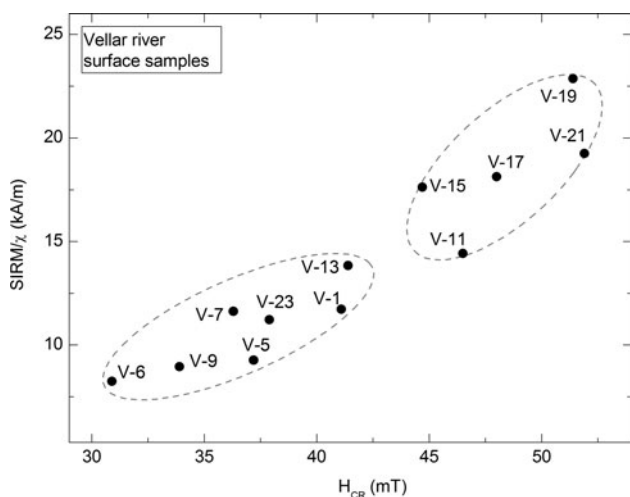


Fig. 4 Scatterplot of $SIRM/\chi$ versus H_{CR} for Vellar (V) samples. Two sample groupings are identified, indicating differences in magnetic mineralogy, e.g., softer magnetic carriers (on the left) belong to sites V-1/5/6/7/9/13/23

some of them. This behavior is coherent with the conclusions of the other related parameters.

The $\kappa_{FD}\%$ parameter is sensitive to the presence of superparamagnetic (SP) material (Dearing et al. 1996). From Bartington Instruments Ltd. (1994) values of $\kappa_{FD}\% > 2.0\%$ indicate virtually no SP grains; those between 2.0 and 10.0% indicate admixtures of SP and coarser non-SP grains; those between 10.0 and 14.0% indicate virtually all SP grains. In Vellar River samples, $\kappa_{FD}\%$ values were below 2.00% in particular; the maximum value was 1.92%. Therefore, the presence of SP grains can be discarded.

Magnetic grain size-dependent parameters (i.e., $SIRM/\chi$, $\kappa_{ARM}-\kappa$ -ratio) and related plots [i.e., King’s plot (Fig. 5a) and Thompson’s plot (Thompson and Oldfield 1986, Fig. 5b)] are in agreement, showing the presence of finer magnetic grain sizes for lower magnetic concentration

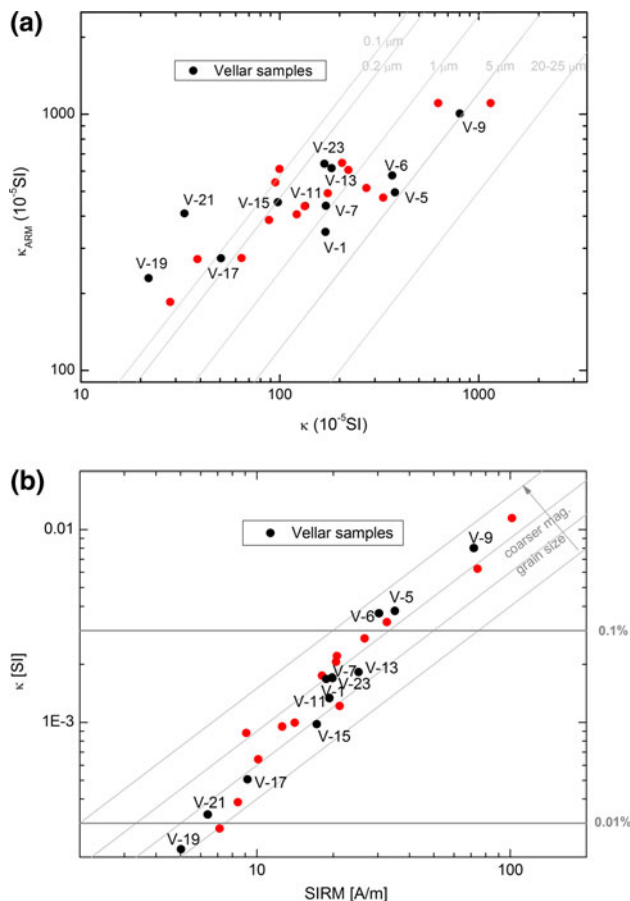


Fig. 5 Two plots using different magnetic parameters. Black dots correspond to samples from the upper layer, and red dots correspond to samples from 30.5 to 91.4 cm. **a** King’s Plot (κ_{ARM} versus κ) for all Vellar (V) samples. As a general trend, samples with higher magnetic concentration-dependent parameters (e.g., V-5, V-6 and V-9) showed coarser magnetic grain sizes. **b** Thompson’s Plot (κ versus $SIRM$) for V samples. The scale of magnetite concentration (%) is displayed on the vertical axis (from Thompson and Oldfield 1986)

samples and vice versa. This trend can also be appreciated in Fig. 2, where higher values of $SIRM/\chi$ correspond to finer magnetic grain sizes.

Magnetic properties of grain size fractions

Values of χ and ARM for various grain sizes fractions of samples V-13-0 and V-23-0 can be observed in Fig. 6a, b. The patterns show similar trends, decreasing towards medium and coarse sand fractions. Higher χ values were found in finer fractions, especially in the fractions of 105 and 63 μm , reaching 879.2 and $1,296.7 \times 10^{-8} \text{ m}^3 \text{ kg}^{-1}$ for samples V-13-0 and V-23-0, respectively.

On the other hand, ferromagnetic concentration-dependent parameters, i.e., ARM and SIRM, also showed a nearly normal distribution for both samples, and their high values were reached for the fraction of 105 μm . As can be noted in Fig. 6a, b, higher ARM values are $2,688.8$ and $1,698.3 \times 10^{-6} \text{ A m}^2 \text{ kg}^{-1}$ for samples V-13-0 and V-23-0, respectively.

Furthermore, magnetite concentrations (estimated from the Thompson's plot) reached high values, up to 0.605 and

0.724%, respectively. Such values are high for finer fractions, especially if they are compared with the sand fractions (0.017 and 0.004% for samples V-13-0 and V-23-0, respectively). Although a granulometric analysis of sand, silt, and clay fractions is not presented here, samples seem to be dominated by fine fractions. The aforementioned magnetic results show that χ is $109.3 \times 10^{-8} \text{ m}^3 \text{ kg}^{-1}$ (Fig. 2) for sample V-13-0, while it is $879.2 \times 10^{-8} \text{ m}^3 \text{ kg}^{-1}$ for finer fractions (Fig. 6a).

The magnetic mineralogy of both samples indicates the presence of magnetite and an extra-magnetic carrier. The influence of fine and coarse fractions in the magnetic signal can be appreciated comparing the H_{CR} distributions (Fig. 6a, b) with their corresponding total values, $H_{CR} = 41.4 \text{ mT}$ (V-13-0) and 51.9 mT (V-23-0). It is possible to conclude from these distributions that different magnetic mineralogy is present in finer (<177 μm) and coarser fractions (>177 μm), the first population being characterized by H_{CR} values between about 31 and 38 mT and the second one with higher H_{CR} values, between 46 and 50 mT. Such differences between magnetic carriers may not only arise from the grain size distribution, but also, as mentioned, from subordinate magnetic carriers.

Magnetic concentration parameters, the uppermost samples from sites V-1 to V-23

Mass-specific susceptibility is a magnetic concentration-dependent parameter, and its values vary according to the kind of magnetic materials, i.e., diamagnetic, paramagnetic, antiferromagnetic and ferrimagnetic materials (typical magnetic properties of natural minerals in, e.g., Maher et al. 1999). As shown in Fig. 2, values of χ ranged from 14.3 to $518.0 \times 10^{-8} \text{ m}^3 \text{ kg}^{-1}$ for samples from the upper layer (surface level). The highest χ values belong to samples V-5-0, V-6-0, and V-9-0. Intermediate values were found for different samples; however, the values decreased towards the river mouth as a general trend (Fig. 2). Other concentration-related remanent parameters, such as ARM and SIRM, are also represented in Fig. 2. They varied between 90.0 and $522.1 \times 10^{-6} \text{ A m}^2 \text{ kg}^{-1}$ for ARM and between 3.3 and $68.5 \times 10^{-3} \text{ A m}^2 \text{ kg}^{-1}$ for SIRM. As can be observed for these remanent parameters, their distribution along the Vellar River is in agreement with the χ distribution.

Assuming magnetite as the main magnetic carrier, magnetite concentration can be estimated from the Thompson's plot. In particular, magnetite concentration varies between 0.007 and 0.382% (see Fig. 5b), showing high contents of this magnetic carrier and a magnetic increase in various sites.

As discussed, high and low χ values are identified along the Vellar River and hence, they can indicate "magnetic

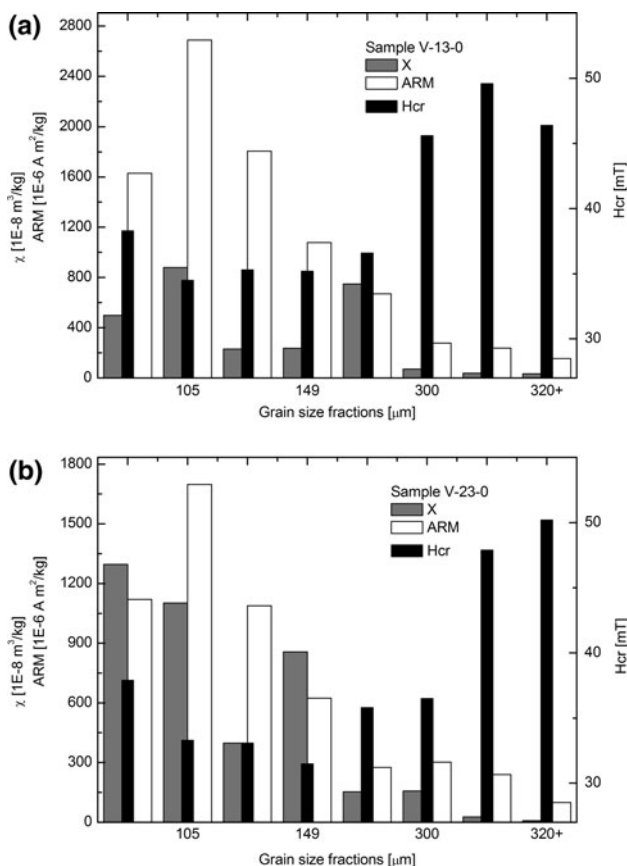


Fig. 6 Results of magnetic concentration-dependent parameters (χ and ARM) and a magnetic carrier-dependent parameter (H_{CR}) for different grain size fractions (from 63 to >320 μm). **a** sample V-13-0 and **b** sample V-23-0

enhancement” in some sites if background mass-specific magnetic susceptibility values between 9.1 and $57.9 \times 10^{-8} \text{ m}^3 \text{ kg}^{-1}$ are considered from Chaparro et al. (2008a). This choice is suitable because the Vellar River is located in the area of influence of the Cauvery and Palaru Rivers (see Fig. 1). All samples belonging to the grouping with harder magnetic carriers (in Fig. 4, on the right (see also Fig. 2), except sample V-11-0, have values below $55.5 \times 10^{-8} \text{ m}^3 \text{ kg}^{-1}$ and therefore they seem to receive a low pollution load. On the other hand, and taking into account this comparison, most samples from the grouping with softer magnetic carriers are interpreted as magnetic enhancement, which is more evident for samples V-5-0, V-6-0, and V-9-0 and moderately evident for samples V-1-0, V-7-0, V-13-0, and V-23-0 (Fig. 2). Such magnetic enhancement may arise from the presence of pollution (an input of magnetic particles and heavy metals produced by industrial and urban activities) or other processes. We ruled out the possibility that the magnetic enhancement is related with natural anomalies on account of the homogeneous chemical composition (Palanivel 2007).

Trace metals

Results of selected metals and the Tomlinson pollution load index are detailed in Table 1. The PLI was computed using Ba, Co, Cr, Cu, Fe, Ni, Pb, V, and Zn and the baseline values were determined from their corresponding minimum values, which can be considered as natural trace metal values in the Vellar River. It is worth mentioning that the baseline values were defined using a reduced number of samples, and such values have a local importance (Vellar sediments). As discussed by a large number of authors (Dudka 1993; Breckenridge and Crockett 1995; Salminen and Tarvainen 1997; Chen et al. 2001; Qian and Lyons 2006), the baseline concentrations depend on the environment, basic geology, type and genesis of the overburden, sample material collected, grain size, and extraction method. There are several involved variables to evaluate the baselines from a dataset; therefore a statistical approach might be necessary. Hence, a detailed geochemical study should be advisable to define the corresponding baselines; however, it is out of the scope of the present contribution.

Although the minimum values belong mainly to samples V-17-0 and V-19-0, similar low values were found in sites V-11, V-15, and V-21. These samples also evidenced low values of magnetic concentration-dependent parameters and harder magnetic carriers. On the other hand, high values above the mean (e.g., 10.3 mg kg^{-1} (Co), 29.9 mg kg^{-1} (Zn), 101.4 mg kg^{-1} (V) and 3.23 g kg^{-1} (Fe) see Table 1) correspond to sites V-1, V-5, V-6, V-9, V-13, and V-23. High levels of some heavy metals could be associated with different human activities in India.

According to Gowd et al. (2010), the main source of chromium is the tannery industry; the presence of copper may be due to activities like steel manufacturing, application of agrochemicals in agro-based production, as well as active untended waste dumps. Vanadium has a wide industrial usage in dyeing, textile, metallurgy, and electronics; and the main sources of zinc are industries and agrochemical products used in agriculture. Another important source of most of these elements could be also related to urban activities and vehicular traffic. Ramasamy et al. (2009) discussed such fact in a preliminary study of a nearby river (Ponnaiyar River).

As concluded, there are differences among sites, which are also evidently appreciated from the PLI values (Table 1). Sites V-1, V-5, V-6, V-9, and V-13 showed higher PLIs (2.60-3.56) than other sites, indicating that they are more influenced by pollution loads.

Vertical distribution

The vertical variation of magnetic parameters and chemical variables was studied for five sites V-5, V-6, V-13, V-19, and V-23. In particular, the results of magnetic susceptibility and PLI showed similar behavior as can be appreciated in Fig. 7. The patterns showed an increasing trend of χ and PLI towards the uppermost sediments. Although such a trend is observed for almost of these sites, sites V-5 and V-13 reached maxima at about 0.6 m and 0.3 m, respectively.

The maxima and minima of both variables coincided very well for all sites, that is, higher values of χ are associated with higher values of PLI (e.g., site V-5), and vice versa (e.g., site V-19). Therefore, mass-specific

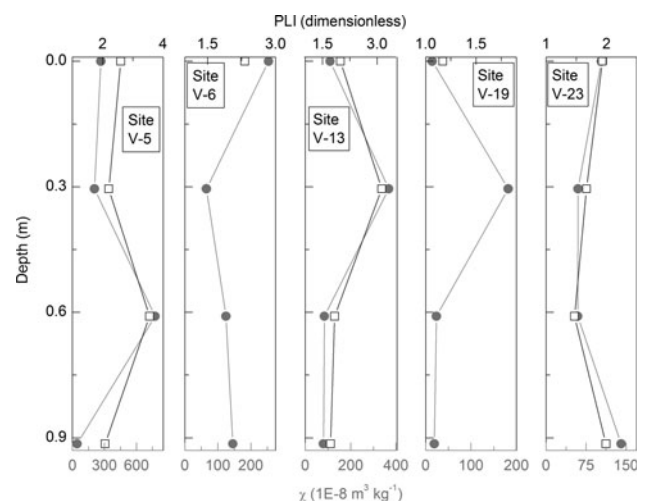


Fig. 7 Vertical variation of magnetic susceptibility and PLI (computed using Ba, Co, Cr, Cu, Fe, Ni, Pb, V and Zn) for five selected Vellar (V) sites

magnetic susceptibility (a magnetic concentration-dependent parameter) may be a useful pollution proxy for this river.

Magnetic and chemical variables

As a first approach, the Pearson correlation coefficients between pairs of variables were obtained; these results are listed in Table 2. Although positive and negative correlations are observed, most of them correspond to significant values up to 0.98. Positive correlations between 0.538 and 0.979 at the 0.05 and 0.01 levels of significance correspond to magnetic concentration-dependent parameters (χ , ARM and SIRM) and to most chemical variables, including Co, Cr, Cu, Fe, V, Zn, and PLI. Relevant parameters are concluded from these results, which are in agreement with previous findings in the study area. On the other hand, there are one-to-one links between magnetic feature-dependent parameters (H_{CR} , $SIRM/\chi$ and κ_{ARM}/κ) and chemical variables, but in this case negative correlations between -0.730 and -0.509 at 0.01 and 0.05 levels of significance were found. If a linear relationship between magnetic and chemical variables is assumed, it is possible to infer that higher concentrations of heavy metals are associated with coarser magnetic grain sizes (e.g., lower values of κ_{ARM}/κ) and softer magnetic carriers (e.g., lower values of H_{CR}).

After these calculations, other multivariate analyses were carried out, namely PCA, CCA, and PCoordA.

For PCA the first three PCs accounted for the 82.5% of the total variance, where PC1 showed a high factor loading of most of the variables (χ , ARM, SIRM, H_{CR} , $SIRM/\chi$, κ_{ARM}/κ , Co, Cr, Cu, Fe, V and Zn). The PC1 demonstrates the main contributions of χ , ARM and SIRM, with loading between 0.85 and 0.91, and chemical variables such as Fe, V, and Zn (with loading between 0.84 and 0.95). The PC2 includes two variables (Ba and Pb), while PC3 only has Ni (with loading 0.70); it was not possible to reconstruct the S -ratio variable with these three PCs. Figure 8 shows the

graphic representation of PC1 and PC2; as can be distinguished some variables are grouped to show a good correlation between them, i.e., χ -V, ARM-SIRM-Zn, Fe-Co, H_{CR} -SIRM/ χ - κ_{ARM}/κ -Cu, and Ba-Pb. Such results are in agreement with the existence of relationships between variables from the correlation analysis.

Next, the canonical R values from CCA were computed, yielding a very good statistically significant canonical correlation, $R^2 = 0.98$ ($p < 0.01$) for this case. On the other hand, magnetic concentration-dependent variables (χ , ARM, SIRM) are closely correlated to chemical variables according to the highest canonical $R^2 = 0.97$ ($p < 0.01$). In contrast, lower canonical correlations ($R^2 = 0.91$, $p = 0.01$; and $R^2 = 0.83$, $p < 0.01$) were found for magnetic feature-dependent variables (S -ratio, H_{CR}) and magnetic grain size-dependent variables (SIRM/ χ , κ_{ARM}/κ), respectively.

From the PCoordA, it was possible to find the existence of a grouping with a homogeneous behavior (Fig. 9).

Finally, the Fuzzy C-means Clustering method was utilized to investigate different (visually) observed groupings from the coordinate PCoordA plane. Four sample groups were used according to the possible grouping observed from PCoordA. To validate this selection of groups, several numbers of groups, from $N = 3$ to $N = 7$, were studied for our data. The optimum number of clusters is four ($N = 4$), which was chosen according to the following priority order: (1) high value of the average silhouette width of each cluster (Kaufman and Rousseeuw 1990); (2) high value of the normalized Dunn's index (Dunn 1973). Each group is characterized by seven magnetic centroids and nine chemical centroids (Table 3) that consider the distance between cases. Although the PLI was not used for calculations in groups Ch, such index is a measure of central tendency that summarizes the behavior of the heavy metal data. Each sample was classified regarding the membership grade; as a rule, a sample belongs to a group if it has a membership grade > 0.7 ;

Table 2 Pearson correlation coefficients between magnetic and chemical variables ($n = 21$) from the Vellar River are listed

Magnetic variable	Chemical variable									
	Ba	Co	Cr	Cu	Fe	Ni	Pb	V	Zn	PLI
χ	0.251	0.721**	0.538*	0.58**	0.800**	0.252	0.391	0.979**	0.801**	0.860**
ARM	0.082	0.815**	0.364	0.383	0.886**	0.198	0.246	0.893**	0.864**	0.800**
SIRM	0.170	0.803**	0.555**	0.573**	0.866**	0.284	0.324	0.975**	0.858**	0.881**
S -ratio	0.255	0.207	0.248	0.258	0.220	0.022	0.137	0.355	0.238	0.307
H_{CR}	-0.484^*	-0.540^*	-0.317	-0.520^*	-0.592^{**}	-0.180	-0.555^{**}	-0.754^{**}	-0.659^{**}	-0.730^{**}
SIRM/ χ	-0.452^*	-0.460^*	-0.306	-0.513^*	-0.496^*	-0.197	-0.509^*	-0.622^{**}	-0.592^{**}	-0.653^{**}
κ_{ARM}/κ	-0.332	-0.587^{**}	-0.471^*	-0.628^{**}	-0.529^*	-0.264	-0.263	-0.607^{**}	-0.632^{**}	-0.680^{**}

Significant correlations are indicated

* Significance at 0.05 level; ** significance at 0.01 level

Fig. 8 Principal component analysis (PCA) using selected magnetic and chemical variables ($m = 16$). The first principal components (Coord 1 and Coord 2) are shown; the circles indicate if variables are reconstructed at 50% (inner circle) or 100% (outer circle). Different grouping of variables are observed, i.e., χ -V, ARM-SIRM-Zn, Fe-Co, H_{CR} -SIRM/ χ - κ_{ARM}/κ -Cu and Ba-Pb

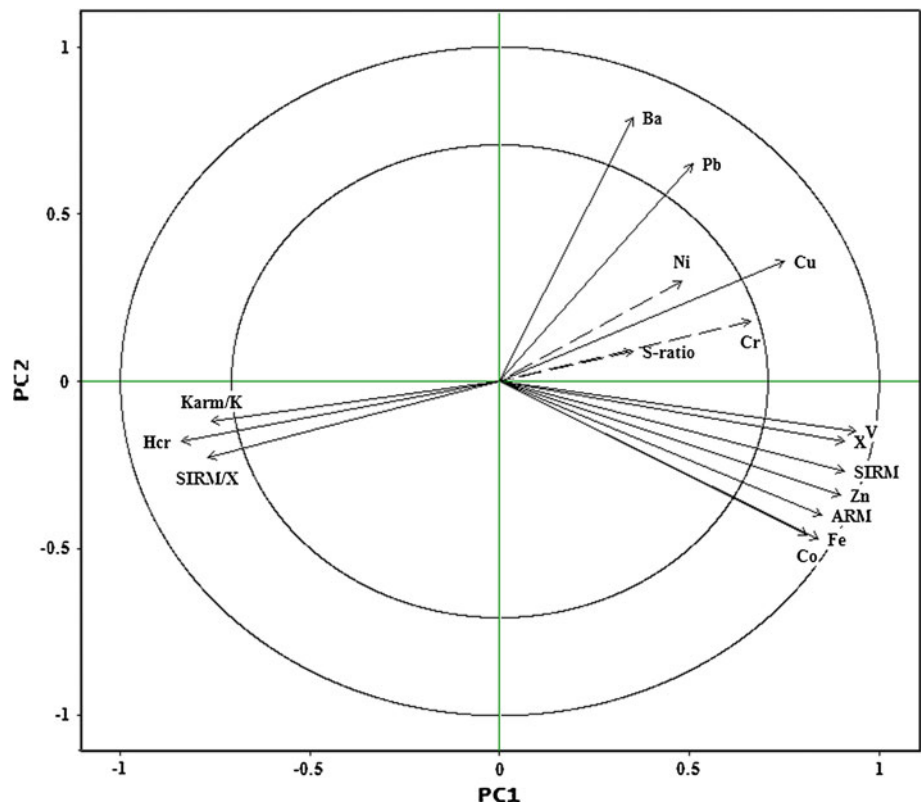


Fig. 9 Principal coordinate analysis (PCoordA) of selected samples ($n = 21$) and selected magnetic and chemical variables ($m = 16$). Individuals are identified and shown in the coordinate plane (Coord 1 and Coord 2). The data classification into four groups, including Group A (less impacted samples), B, C, and D (most impacted samples), was obtained from the fuzzy C-means cluster analysis

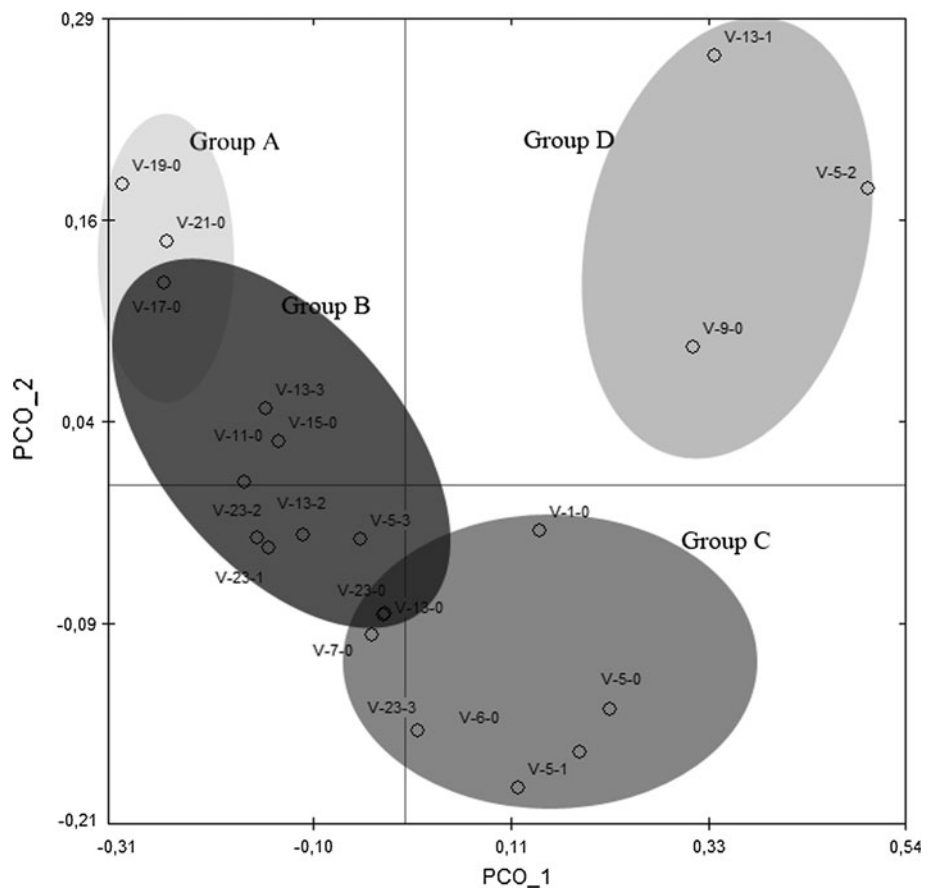


Table 3 Results from the fuzzy C-means cluster analysis

Variable	1	2	3	4
M classification				
χ ($1\text{E-}8 \text{ m}^3 \text{ kg}^{-1}$)	148.5	549.4	23.2	75.8
ARM ($1\text{E-}6 \text{ A m}^2 \text{ kg}^{-1}$)	239.7	460.9	146.8	185.9
SIRM ($1\text{E-}3 \text{ A m}^2 \text{ kg}^{-1}$)	15.3	51.0	4.3	10.8
S-ratio (dimensionless)	0.94	0.96	0.94	0.94
H_{CR} (mT)	37.5	32.3	51.1	43.8
SIRM/ χ (kA/m)	10.9	9.5	20.6	15.1
$\kappa_{\text{ARM}}/\kappa$ (dimensionless)	2.76	1.29	10.79	3.94
Ch classification				
Ba (ppm)	307.98	254.09	259.69	231.55
Co (ppm)	10.91	6.93	9.94	21.36
Cr (ppm)	431.19	275.91	316.53	470.00
Cu (ppm)	15.89	8.91	10.89	14.29
Fe (%)	3.38	1.90	2.81	8.66
Ni (ppm)	36.86	27.02	27.80	41.91
Pb (ppm)	8.38	6.09	5.36	6.91
V (ppm)	122.20	65.65	86.68	182.05
Zn (ppm)	33.71	17.44	26.86	68.25
PLI (dimensionless)	2.43	1.46	1.85	3.46

Four centroids for each variable from the magnetic (M) and chemical (Ch) groups are detailed. The PLI was not used for calculations in groups Ch, but it is shown here as a representative variable (measure of central tendency) of heavy metal data

otherwise, the sample belongs to two (or more) groups. In the latter case, the sample has a shared membership and the most relevant group is denoted using the symbol +. For example, if group 1 is the most relevant among others the sample is classified as 1+. Taking into account these rules, M and Ch classifications were obtained for each sample (Table 4).

Subsequently, four M groups obtained by classification (Table 3) were fixed, and their possible combinations with each Ch group were examined for all samples. These combinations were linked from Table 4, defining the following four new groups: A, B, C, and D (Fig. 9):

- Group A (M3-Ch2) is characterized by the lowest values of chemical variables (e.g., PLI = 1.46, see also Table 3) and magnetic concentration-dependent variables (e.g., $\chi = 23.2 \times 10^{-8} \text{ m}^3 \text{ kg}^{-1}$) and by the highest values of magnetic feature/grain size-dependent variables (e.g., $\kappa_{\text{ARM}}/\kappa = 10.79$).
- Group B (M4-Ch3, M4-Ch2), with relation to group A, shows an increase of chemical (e.g., PLI = 1.85 and 1.46) and magnetic concentration-dependent variables (e.g., $\chi = 75.8 \times 10^{-8} \text{ m}^3 \text{ kg}^{-1}$) and a decrease of magnetic feature/grain size-dependent variables (e.g., $\kappa_{\text{ARM}}/\kappa = 3.94$).

- Group C (M1-Ch1, M1-Ch3) is characterized by lower values of magnetic feature/grain size-dependent variables (e.g., $\kappa_{\text{ARM}}/\kappa = 2.76$) and by higher values of chemical variables (e.g., PLI = 2.43 and 1.85) and magnetic concentration-dependent variables (e.g., $\chi = 148.5 \times 10^{-8} \text{ m}^3 \text{ kg}^{-1}$).
- Group D (M2-Ch4, M2-Ch1), in contrast to the first group, shows the highest values of chemical variables (e.g., PLI = 3.46 and 2.43) and magnetic concentration-dependent variables (e.g., $\chi = 549.4 \times 10^{-8} \text{ m}^3 \text{ kg}^{-1}$), and minimum values of magnetic feature/grain size-dependent variables (e.g., $\kappa_{\text{ARM}}/\kappa = 1.29$).

This classification allows us to identify several clusters of samples that are characterized by different magnetic properties and heavy metals' loading, and thus to determine the pollution influence in different sites.

Conclusions

- Samples are dominated by ferrimagnetic minerals corresponding to magnetite-like minerals, but minor contributions of antiferromagnetic minerals are also expected in different sites. As a first approach, for the magnetic parameters, samples seem to be grouped into two groupings: (a) one with softer magnetic carriers and higher magnetic concentrations and (b) another one with lower magnetic concentration and harder/finer magnetic carriers than the first one.
- Magnetic properties of grain size fractions show a normal-like distribution, reaching the highest values of magnetic concentration-dependent parameters for finer fractions. In addition, the magnetic mineralogy is slightly different between the fine fractions ($H_{\text{CR}} = 31\text{--}38 \text{ mT}$) and coarse fractions ($H_{\text{CR}} = 46\text{--}50 \text{ mT}$).
- Magnetite concentration varied between 0.007 and 0.382%, showing high contents of this magnetic mineral and a magnetic enhancement in various sites, which was more evident for sites V-5, V-6, and V-9 and more moderate for sites V-1, V-7, V-13, and V-23. Such magnetic enhancement may arise from the presence of pollution, in which there is an input of magnetic particles and heavy metals produced by industrial and urban activities or other process.
- The vertical variation of magnetic susceptibility and PLI showed a very good agreement between both patterns and an increasing trend of both parameters towards the uppermost sediments.
- Positive correlations (R values from 0.538 to 0.979) between magnetic concentration-dependent parameters and most chemical variables prove the relationship

Table 4 Fuzzy C-means cluster classification

Sample	M					Ch				
	Group 1	Group 2	Group 3	Group 4	Classification	Group 1	Group 2	Group 3	Group 4	Classification
V-1-0	0.590	0.025	0.030	0.356	1+	0.427	0.151	0.202	0.220	1+
V-5-0	0.693	0.094	0.040	0.174	1+	0.829	0.053	0.078	0.040	1
V-5-1	0.396	0.235	0.111	0.257	1+	0.452	0.181	0.324	0.043	1+
V-5-2	0.091	0.808	0.038	0.063	2	0.286	0.099	0.136	0.478	4+
V-5-3	0.125	0.017	0.060	0.799	4	0.507	0.203	0.218	0.072	1+
V-6-0	0.509	0.236	0.064	0.191	1+	0.802	0.058	0.118	0.021	1
V-7-0	0.690	0.046	0.039	0.226	1+	0.029	0.127	0.837	0.006	3
V-9-0	0.016	0.970	0.005	0.009	2	0.373	0.133	0.269	0.225	1+
V-11-0	0.279	0.052	0.118	0.551	4+	0.065	0.513	0.402	0.020	2+
V-13-0	0.431	0.026	0.034	0.509	4+	0.126	0.192	0.656	0.026	3+
V-13-1	0.204	0.629	0.048	0.118	2+	0.044	0.027	0.038	0.891	4
V-13-2	0.060	0.005	0.010	0.926	4	0.031	0.183	0.778	0.008	3
V-13-3	0.156	0.037	0.140	0.667	4+	0.124	0.327	0.511	0.038	3+
V-15-0	0.082	0.014	0.066	0.839	4	0.075	0.230	0.666	0.029	3+
V-17-0	0.129	0.029	0.261	0.581	4+	0.088	0.485	0.386	0.040	2+
V-19-0	0.024	0.009	0.917	0.049	3	0.056	0.722	0.201	0.021	2
V-21-0	0.027	0.011	0.911	0.050	3	0.024	0.851	0.117	0.007	2
V-23-0	0.822	0.020	0.020	0.139	1	0.086	0.206	0.679	0.029	3+
V-23-1	0.284	0.031	0.082	0.603	4+	0.056	0.671	0.261	0.012	2+
V-23-2	0.507	0.039	0.066	0.388	1+	0.088	0.637	0.246	0.029	2+
V-23-3	0.686	0.065	0.047	0.202	1+	0.141	0.297	0.530	0.032	3+

Membership values for all four magnetic (M) and chemical (Ch) groups and the corresponding data classification. A sample belongs to a group if it has a membership grade >0.7; otherwise, the most relevant group is denoted using the symbol +

between both kinds of variables. In this study, χ , ARM and SIRM seem to be relevant parameters to describe Co, Cr, Cu, Fe, V, Zn, and PLI. This fact is also supported by CCA, where the highest canonical correlation (canonical $R^2 = 0.97, p < 0.01$) was found between concentration-dependent parameters and chemical variables. Furthermore, PCA indicated that some variables are grouped and show a good correlation between them, i.e., χ -V, ARM-SIRM-Zn, Fe-Co, H_{CR} -SIRM/ χ - κ_{ARM} / κ -Cu.

- The PCoordA and Fuzzy C-means Clustering method yielded successful results that allowed us to obtain a data classification according to the degree of contamination. In particular, a fuzzy clustering and four groups were accomplished. Thus, less impacted samples (e.g., sites V-17 and V-19) belong to Group A, while, in contrast, the most impacted ones (e.g., sites V-5 and V-9) belong to Group D.

Acknowledgments The authors wish to thank the Annamalai University, Paavai Engineering College, Universidad Nacional del Centro de la Provincia de Buenos Aires (UNCPBA), and National Council for Scientific and Technological Research (CONICET) for their financial support. The authors thank both reviewers for their constructive comments and suggestions.

References

Bartington Instruments Ltd (1994) Operation manual. Environmental magnetic susceptibility—Using the Bartington MS2 system. Chi Publishing, UK, p 54

Beckwith P, Ellis J, Revitt D, Oldfield F (1986) Heavy metal and magnetic relationships for urban source sediments. *Phys Earth Planet Int* 42:67–75

Breckenridge RP, Crockett AB (1995) Determination of background concentrations of inorganics in soils and sediments at hazardous waste sites. EPA/540/S-96/500, Washington, DC

Chaparro MAE, Bidegain JC, Sinito AM, Gogorza CS, Jurado S (2004) Magnetic studies applied to different environments (soils and stream-sediments) from a relatively polluted area in Buenos Aires Province, Argentina. *Environ Geol* 45(5):654–664

Chaparro MAE, Lirio JM, Nuñez H, Gogorza CSG, Sinito AM (2005) Preliminary magnetic studies of lagoon and stream sediments from Chascomús Area (Argentina)—magnetic parameters as pollution indicators and some results of using an experimental method to separate magnetic phases. *Environ Geol* 49(1):30–43

Chaparro MAE, Gogorza CSG, Chaparro MAE, Irurzun MA, Sinito AM (2006) Review of magnetism and heavy metal pollution studies of various environments in Argentina. *Earth Planets Space* 58(10):1411–1422

Chaparro MAE, Sinito AM, Ramasamy V, Marinelli C, Chaparro MAE, Mullainathan S, Murugesan S (2008a) Magnetic measurements and pollutants of sediments from Cauvery and Palaru River, India. *Environ Geol* 56:425–437

Chaparro MAE, Chaparro MAE, Marinelli C, Sinito AM (2008b) Multivariate techniques as alternative statistical tools applied to

- magnetic proxies for pollution: cases of study from Argentina and Antarctica. *Environ Geol* 54:365–371
- Chen M, Ma LQ, Hoogeweg CG, Harris WG (2001) Arsenic background concentrations in Florida, U.S.A. Surface soils: Determination and interpretation. *Environmental Forensics* 2:117–126
- Cuadras CM (1981) *Métodos de analisis multivariante*, Eunibar, Barcelona
- Dearing J, Dann R, Hay K, Lees J, Loveland P, Maher B, O'Grady K (1996) Frequency-dependent susceptibility measurements of environmental materials. *Geophys J Int* 124:228–240
- Desenfant F, Petrovský E, Rochette P (2004) Magnetic signature of industrial pollution of stream sediments and correlation with heavy metals: case study from South France. *Water Air Soil Pollut* 152(1):297–312
- Dudka S (1993) Baseline concentrations of As, Co, Cr, Cu, Ga, Mn, Ni, and Se in surface soils. *Pol Appl Geochem* 2:23–28
- Dunn JC (1973) A fuzzy relative of the ISODATA process and its use in detecting compact well-separated clusters. *J Cybern* 3:32–57
- Gowd SS, Reddy MR, Govil PK (2010) Assessment of heavy metal contamination in soils at Jajmau (Kanpur) and Unnao industrial areas of the Ganga Plain, Uttar Pradesh, India. *J Hazard Mater* 174(1–3):113–121
- Hunt A, Jones J, Oldfield F (1984) Magnetic measurements and heavy metals in atmospheric particulates of anthropogenic origin. *Sci Total Environ* 33:129–139
- InfoStat (2009) *InfoStat versión 2009*. Grupo InfoStat, FCA. Universidad Nacional de Córdoba, Argentina
- Jain SK, Agarwal PK, Singh VP (2007) *Hydrology and water resources of India*. Ed. Springer, Dordrecht, The Netherlands, pp 1258
- Jordanova DV, Hoffmann V, Thomas Fehr K (2004) Mineral magnetic characterization of anthropogenic magnetic phases in the Danube river sediments (Bulgarian part). *Earth Planet Sci Lett* 221:71–89
- Kaufman L, Rousseeuw PJ (1990) *Finding groups in data: an introduction to cluster analysis*. Wiley, New York
- King J, Banerjee SK, Marvin J, Özdemir Ö (1982) A comparison of different magnetic methods for determining the relative grain size of magnetite in natural materials: Some results from lake sediments. *Earth Planet Sci Lett* 59:404–419
- Knab M, Hoffmann V, Petrovský E, Kapicka A, Jordanova N, Appel E (2006) Surveying the anthropogenic impact of the Moldau river sediments and nearby soils using magnetic susceptibility. *Environ Geol* 49:527–535
- Maher BA, Thompson R, Hounslow MW (1999) Introduction. In: Maher BA, Thompson R (eds) *Quaternary climate, environments and magnetism*. Cambridge University Press, Cambridge, pp 1–48
- Palanivel S (2007) Regional geological setting and major geochemical pattern of Upper Agniar and Vellar Basins, Tamil Nadu. In: Rajedran S et al (eds) "Mineral exploration: recent strategies". New India Publishing Agency, New Delhi, pp 213–222
- Peters C, Dekkers M (2003) Selected room temperature magnetic parameters as a function of mineralogy, concentration and grain size. *Phys Chem Earth* 28:659–667
- Petrovský E, Ellwood B (1999) Magnetic monitoring of air, land and water pollution. In: Maher BA, Thompson R (eds) *Quaternary climates, environment and magnetism*. Cambridge University Press, Cambridge, pp 279–322
- Petrovský E, Kapicka A, Jordanoa N, Knob M, Hoffmann V (2000) Low field susceptibility: a proxy method of estimating increased pollution of different environmental systems. *Environ Geol* 39(3–4):312–318
- Qian SS, Lyons RE (2006) Characterization of background concentrations of contaminants using a mixture of normal distributions. *Environ Sci Technol* 40:6021–6025
- R version 2.9.2 (2009-08-24) © (2009) The R Foundation for Statistical Computing [<http://www.r-project.org/>] ISBN 3-900051-07-0
- Ramasamy V, Murugesan S, Mullainathan S, Chaparro MAE (2006) Magnetic characterization of recently excavated sediments of Cauvery river, Tamilnadu, India. *Pollut Res* 25(2):357–362
- Ramasamy V, Suresh G, Venkatachalapathy R (2009) Magnetic susceptibility of the Ponnaiyar river sediments, Tamilnadu, India. *Global J Environ Res* 3(2):126–131
- Salminen R, Tarvainen T (1997) The problem of defining geochemical baselines. A case study of selected elements and geological materials in Finland. *J Geochem Explor* 60:91–98
- Scholger R (1998) Heavy metal pollution monitoring by magnetic susceptibility measurements applied to sediments of the river Mur (Styria, Austria). *Eur J Environ Eng Geophys* 3:25–37
- Thompson R, Oldfield F (1986) *Environmental magnetism*. Allen & Unwin (Publishers) Ltd, London, p 225
- Tomlinson DL, Wilson JG, Harris CR, Jeffrey DW (1980) Problems in the assessment of heavy metals levels in estuaries and the formation of a pollution index. *Helgol Meeresunters* 33:566–575
- Yang T, Liu Q, Chan L, Liu Z (2007) Magnetic signature of heavy metal pollution of sediments: case study from the East Lake in Wuhan, China. *Environ Geol* 52:1639–1650